Journal of Biomedical and Translational Research
pISSN 2508-1357 eISSN 2508-139X

Original Article
J Biomed Transl Res 2025;26(4):107-122
https://doi.org/10.12729/jbtr.2025.26.4.107

Biocompatibility evaluation of titanium nitride coating for canine patellar groove implant

Yangwon Chae[1,2†], Euisin Yang[1,2†], Taehwan Kim[1,2], Hyunmin Jo[1,2], Dong-Hyun Kim[3], Byeonghak Kim[3], Kyung Mi Shim[1,2], Se Eun Kim[1,2*], Seong Soo Kang[1,2*]

[1]*Department of Veterinary Surgery, College of Veterinary Medicine and BK21 Plus Project Team, Chonnam National University, Gwangju 61186, Korea*
[2]*Biomaterial R&BD Center, Chonnam National University, Gwangju 61186, Korea*
[3]*Doiff Co., Ltd., Suncheon 58021, Korea*

Received: Nov 3, 2025
Revised: Nov 18, 2025
Accepted: Nov 20, 2025

†These authors contributed equally to this work.

***Corresponding author**
Se Eun Kim
Department of Veterinary Surgery, College of Veterinary Medicine and BK21 Plus Project Team, Chonnam National University, Gwangju 61186, Korea
Tel: +82-62-530-2812
E-mail: ksevet@jnu.ac.kr

Seong Soo Kang
Department of Veterinary Surgery, College of Veterinary Medicine and BK21 Plus Project Team, Chonnam National University, Gwangju 61186, Korea
Tel: +82-62-530-2877
E-mail: vetkang@chonnam.ac.kr

ORCID
Yangwon Chae
https://orcid.org/0000-0002-1471-8836
Euisin Yang
https://orcid.org/0000-0001-6789-2726
Taehwan Kim
https://orcid.org/0009-0008-1050-9560

Abstract

Medial patellar luxation is a common orthopedic disorder in dogs, and advanced cases with severe skeletal deformities or femoropatellar osteoarthritis are often unresponsive to conventional techniques. Patellar groove replacement (PGR) has been proposed as an alternative surgical option; however, systematic comparisons of coating technologies for veterinary PGR implants remain limited. This study aimed to evaluate the physicochemical properties, biological compatibility, and functional performance of a newly developed titanium nitride (TiN)–coated PGR system compared with a clinically available amorphous diamond-like carbon (ADLC)–coated device. TiN-coated prototypes were fabricated using Ti-6Al-4V alloy by injection molding combined with arc ion plating, which requires simpler equipment and lower production costs than the vacuum plasma deposition used for ADLC. Physicochemical evaluations, including corrosion resistance, hardness, surface roughness, and coating thickness, were conducted following International Organization for Standardization (ISO) and Korean Industrial Standards (KS) guidelines. *In vitro* biocompatibility was assessed using MTT and cell adhesion assays with L-929 fibroblasts, while inflammatory cytokine profiling (interleukin [IL]-1β and IL-6) in a rat subcutaneous model was used to evaluate local tissue responses. Functional feasibility was examined in a canine femoral model bilaterally implanted with TiN- or ADLC-coated PGR systems and monitored for one year through clinical, radiographic, computed tomography (CT), magnetic resonance imaging , and micro-CT assessments. Both coatings demonstrated excellent corrosion resistance and absence of cytotoxicity. TiN-coated implants showed slightly greater hardness and coating thickness, with comparable surface roughness and biocompatibility. All implants maintained stable fixation, proper patellar tracking, and satisfactory bone–implant integration. These findings indicate that TiN-coated PGR implants achieve biological and mechanical performance equivalent to ADLC devices while offering advantages in manufacturing simplicity, scalability, and cost-efficiency, supporting their clinical applicability in veterinary orthopedics.

Keywords: titanium; carbon; surface properties; patella; arthroplasty

Hyunmin Jo
https://orcid.org/0000-0002-5391-1911
Dong-Hyun Kim
https://orcid.org/0009-0005-5124-1722
Byeonghak Kim
https://orcid.org/0009-0001-3561-3785
Kyung Mi Shim
https://orcid.org/0000-0002-2273-6655
Se Eun Kim
https://orcid.org/0000-0001-6626-0786
Seong Soo Kang
https://orcid.org/0000-0002-8957-0354

Conflict of Interest
No potential conflict of interest relevant to this article was reported.

Acknowledgements
This research was supported by the Technology Innovation Program (or Industrial Strategic Technology Development Program) (20017903, Development of medical combination device for active precise delivery of embolic beads for transcatheter arterial chemoembolization and simulator for embolization training to cure liver tumor) funded by the Ministry of Trade, Industry & Energy (MOTIE, Republic of Korea).

Ethics Approval
The animal study was approved by the Institutional Animal Care and Use Committee of Chonnam National University in Korea (Approval No. CNU IACUC-YB-2022-32, CNU IACUC-2023-03).

INTRODUCTION

Patellar luxation is a common orthopedic disorder in dogs, especially in small breeds, with medial patellar luxation (MPL) being much more prevalent than lateral luxation. The prevalence of MPL has been reported to reach 9.8% in some populations, underscoring its clinical relevance. The etiology of MPL is multifactorial and developmental, involving congenital skeletal deformities and periarticular soft tissue abnormalities [1–3]. In severe cases, especially grades III and IV, pronounced angular deformities such as distal femoral varus, femoral torsion, and procurvatum disrupt the quadriceps mechanism, leading to chronic patellar instability. Over time, adaptive changes such as medial retinacular contracture and quadriceps muscle atrophy worsen maltracking, accelerate trochlear wear, and contribute to secondary femoropatellar osteoarthritis [3–5].

Conventional surgical approaches such as trochleoplasty, tibial tuberosity transposition, and soft tissue balancing generally provide satisfactory results in low-grade MPL but are often insufficient in advanced cases with significant skeletal malalignment [6–8]. Corrective femoral osteotomies have therefore been proposed; however, these procedures remain technically demanding, rely heavily on precise preoperative planning, and carry a risk of complications [9, 10]. Given these limitations, patellar groove replacement (PGR) has been introduced as an alternative strategy for complicated cases, including severe femoropatellar osteoarthritis, trochlear dysplasia, and failed prior surgeries. By replacing the native trochlear groove with a prosthetic component, PGR aims to restore stable patellar tracking, preserve joint motion, and minimize articular wear [11–15].

Advances in implant design and surface engineering have further expanded the potential of PGR. Surface coatings such as amorphous diamond-like carbon (ADLC) and titanium nitride (TiN) have been developed to improve wear resistance, corrosion resistance, and biocompatibility. ADLC coatings, composed of amorphous carbon with mixed sp^3 and sp^2 bonding, exhibit extremely high hardness, excellent corrosion resistance, and a very low friction coefficient, which helps minimize wear and extend implant longevity. These properties have established ADLC as an effective surface treatment for orthopedic and dental implants in both human and veterinary applications [16–20]. However, several limitations restrict its widespread clinical adoption. ADLC coatings often suffer from weak adhesion to metallic substrates due to internal residual stress, require high-vacuum plasma deposition systems with complex multistep processing, and involve high manufacturing costs. In addition, coating uniformity and durability can be difficult to maintain on complex implant geometries, and delamination may occur under cyclic mechanical loading [21, 22].

In contrast, TiN coatings can be fabricated through arc ion plating combined with injection-molded Ti-6Al-4V substrates, requiring simpler facilities and lower production costs than ADLC deposition processes. TiN offers excellent corrosion resistance, favorable wear properties, strong coating adhesion, and consistent thickness control, making it an attractive and scalable alternative for veterinary implants [23–27].

Despite these advantages, veterinary-specific standards for evaluating implant coatings are

https://doi.org/10.12729/jbtr.2025.26.4.107

lacking, and most devices are still assessed using benchmarks designed for human orthopedic systems. International Organization for Standardization (ISO) standards for implant materials, biocompatibility, and wear testing provide useful guidance, but their direct application to the unique biomechanical environment of quadrupedal locomotion remains challenging [28]. Furthermore, few comparative studies have investigated how surface coating materials influence the clinical feasibility and long-term safety of PGR systems in companion animals.

Based on these limitations, we evaluated a newly developed TiN-coated PGR system as a practical and cost-effective alternative to an existing ADLC-coated device. Comprehensive physicochemical, *in vitro*, and *in vivo* evaluations were conducted to verify the biological performance, mechanical reliability, and manufacturing advantages of the TiN-coated system for veterinary orthopedic applications.

MATERIALS AND METHODS

Implant materials

Two PGR systems were evaluated: a TiN-coated prototype (Doiff, Suncheon, Korea) and a clinically available ADLC-coated predicate device (KYON, Zürich, Switzerland; Fig. 1). Both systems consisted of a femoral base plate and an artificial trochlear groove component secured with orthopedic screws (Doiff) and were sterilized with ethylene oxide prior to implantation.

The TiN-coated prototypes were fabricated from Ti-6Al-4V alloy using an injection-molding route followed by arc ion plating. After molding, the substrates underwent sequential ultrasonic cleaning in acetone and ethanol for 10 min each and were vacuum-dried before coating. The components were then placed in an arc ion plating chamber and degassed to 3.0×10^{-5} torr. For surface activation, high-purity argon was introduced to a working pressure of 10–20 mTorr, and a 900 W plasma was applied for 10 min to remove residual surface contaminants through ion bombardment. Following evacuation, nitrogen gas was introduced under the same pressure range, and TiN deposition was performed using a cathodic arc source operated at an arc current of 60–80 A. During coating, the substrate temperature was maintained at 250°C–350°C, and the deposition time (typically 40–60 min) was adjusted to achieve uniform film growth. These coating conditions consistently produced TiN layers with strong adhesion and

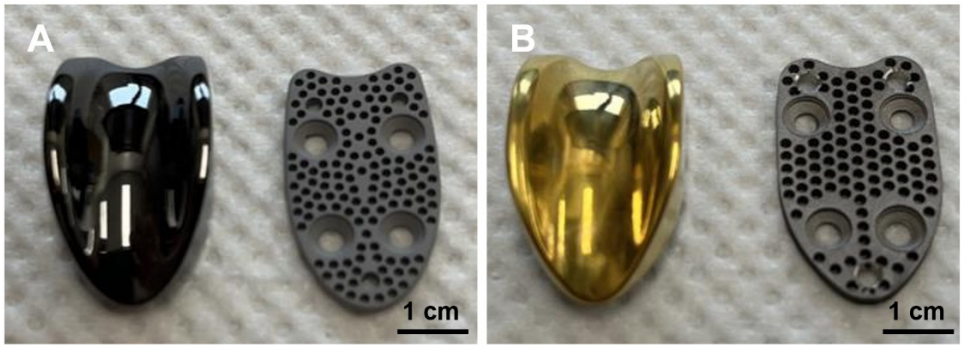

Fig. 1. Representative images of the patellar groove replacement (PGR) systems. (A) Amorphous diamond-like carbon (ADLC)-coated predicate device showing a black trochlear groove surface. (B) Titanium nitride (TiN)-coated prototype with a golden surface finish.

uniform thickness (1.69–1.73 μm) while requiring substantially simpler equipment and lower processing temperatures compared with the CNC machining and high-vacuum plasma deposition used for ADLC coating.

Physicochemical property tests

Physicochemical characterization included neutral salt spray, surface hardness, surface roughness, and coating thickness measurements. The neutral salt spray test was performed according to Korean Industrial Standards (KS) D 9502:2020 for 96 hr at 35 ± 2°C using a 5% NaCl solution.

Surface hardness was measured with a nano-indentation tester (NHT2, Anton Paar, Graz, Austria) equipped with a Berkovich indenter, following ISO 14577-4:2016. Each material was tested five times under identical conditions (maximum load: 50 mN; approach speed: 2,000 nm/min; dwell time: 5 s; loading/unloading rate: 100 mN/min). Surface roughness (Ra, Rz) was measured with a contact profilometer (SJ-210, Mitutoyo, Kawasaki, Japan) in accordance with KS B ISO 4287:2014.

Coating thickness was determined using a ball cratering test (Calotest Compact, CSM Instruments, Peseux, Switzerland) based on KS I 0051:1999. All measurements were performed in quintuplicate (n = 5 per group). One-way ANOVA was used for statistical analysis ($^{*}p<0.05$).

In vitro implant evaluation

Cytotoxicity test

Cytotoxicity was assessed according to ISO 10993-5 using the MTT assay in L-929 mouse fibroblasts (KCLB, Seoul, Korea). Five experimental groups were prepared: control, negative control, positive control, ADLC-coated, and TiN-coated. Extracts were prepared in minimum essential medium (Gibco, Thermo Fisher Scientific, Waltham, MA, USA) and applied to cells in 96-well plates. After 24-hr incubation, optical density (OD) was measured at 570 nm using a microplate reader (SpectraMax i3x, Molecular Devices, San Jose, CA, USA). Cell viability (%) was calculated using the following formula:

$$\text{Cell viability (\%)} = 100 \times \frac{\text{OD570e}}{\text{OD570b}} \quad (1)$$

Values below 70% were considered cytotoxic. One-way ANOVA was used for statistical analysis ($^{**}p<0.01$, $^{***}p<0.001$).

Cell activity test

Cell adhesion and proliferation were assessed using discs prepared from stainless steel (control), uncoated Ti-6Al-4V, and TiN-coated Ti-6Al-4V. Discs (15-mm diameter, 1-mm thickness) were placed in 24-well plates, and L-929 cells were seeded at a density of 2×10^4 cells/well. After incubation for 4 hr or 24 hr, viable cells were quantified using a hemocytometer under an inverted microscope (CKX53, Olympus, Tokyo, Japan).

https://doi.org/10.12729/jbtr.2025.26.4.107

In vivo inflammatory response test in rats

Animals

All animal procedures were approved by the Institutional Animal Care and Use Committee (IACUC) of Chonnam National University (Approval No. CNU IACUC-YB-2022-32). Nine 7-week-old male Sprague–Dawley rats (190–230 g; Samtaco Bio Korea, Osan, Korea) were housed in an Association for Assessment and Accreditation of Laboratory Animal Care (AAALAC)-accredited facility under controlled temperature (23 ± 2°C) and humidity (60 ± 10%), with a 12-hr light/dark cycle. Rats were provided with free access to water and standard chow (Samyang Feed, Incheon, Korea).

Sample preparation and implantation

Disc-shaped samples (16.4 ± 0.1-mm outer diameter, 1.5-mm inner diameter, 1.0-mm thickness) were prepared in four types: untreated Ti-6Al-4V, etched Ti-6Al-4V, TiN-coated, and ADLC-coated. Under general anesthesia (xylazine 10 mg/kg IM; tiletamine–zolazepam 30 mg/kg IM), a 2-cm dorsal midline incision was made, and one disc was implanted subcutaneously over the fascia in each rat. Wounds were closed with absorbable sutures (Surgisorb, Samyang Biopharm, Seoul, Korea).

Sampling and cytokine analysis

At 4 weeks post-implantation, rats were anesthetized as described above, and 2 mL of blood was collected via cardiac puncture into EDTA tubes. Plasma was obtained by centrifugation (848 g, 20 min, 4°C; Hanil Micro 17R, Hanil Scientific, Daejeon, Korea) and stored at –20°C until analysis. Plasma concentrations of interleukin (IL)-1β and IL-6 were quantified using rat-specific ELISA kits (R&D Systems, Minneapolis, MN, USA).

In vivo preclinical studies in dogs

Animals

Two healthy male beagles (14–16 months, ~10 kg) were used in this preclinical evaluation, which was approved by the IACUC of Chonnam National University (Approval No. CNU IACUC-2023-03). Animals were housed in an AAALAC-accredited facility under controlled environmental conditions (temperature 23 ± 2°C, humidity 60 ± 10%, 12-hr light/dark cycle) with *ad libitum* access to filtered water and a commercial diet (Lotte-Nestlé Purina, Cheongju, Korea).

Surgical planning and procedures

Preoperative implant sizing was based on radiographic measurements, and surgical planning was performed using veterinary orthopedic software (ver. 2.8.2, VETSOS Education, London, UK).

To enable comparative evaluation, Dog 1 received a TiN-coated prototype in the right stifle and a clinically available ADLC-coated device in the left stifle. Dog 2 received bilateral TiN-coated implants, and a tibial plateau leveling osteotomy (TPLO) was additionally per-

formed on the left stifle to simulate complex orthopedic conditions.

Premedication included glycopyrrolate (0.005 mg/kg, subcutaneously [SC]; Reyon, Seoul, Korea), famotidine (0.5 mg/kg, intravenously [IV]; Dong-A ST, Seoul, Korea), cefazolin (20 mg/kg, IV; Hankook Korus Pharm, Seoul, Korea), and medetomidine (0.01 mg/kg, intramuscularly; Provet, Victoria, Australia). Analgesia was provided with carprofen (2.2 mg/kg, SC; Zoetis, Parsippany, NJ, USA), tramadol (5 mg/kg, IV; Huons, Seongnam, Korea), and continuous ketamine infusion (10 μg/kg/min; Yuhan, Seoul, Korea). General anesthesia was induced with alfaxalone (1.5 mg/kg, IV; Zoetis) and maintained with isoflurane (2%–3%; Baxter, Deerfield, IL, USA).

Dogs were positioned in dorsal recumbency. Both hindlimbs were shaved and disinfected with 10% povidone-iodine and 70% ethanol. A longitudinal skin incision was made on the cranial aspect of the stifle joint. After joint exposure, two Kirschner wires were inserted approximately 2 mm below the trochlear groove to guide osteotomy using an oscillating saw (DePuy Synthes, Raynham, MA, USA). The native trochlear groove was resected with caution to avoid injury to the extensor digitorum longus muscle.

The femoral base plate of the PGR system was implanted into the prepared femoral surface, followed by fixation of the artificial patellar groove component to the base plate with orthopedic screws (Fig. 2). In the left hindlimb of Dog 2, TPLO was performed as pre-planned; the proximal tibia was rotated to achieve the desired tibial plateau angle and stabilized using a TPLO plate (Orthomed, Huddersfield, UK).

Postoperative care and follow-up evaluations

Postoperative medications were administered for 7 days and included famotidine (1 mg/kg PO; Dong-A ST), enrofloxacin (5 mg/kg per os [PO]; Bayer, Leverkusen, Germany), carprofen (4.4 mg/kg PO; Zoetis), gabapentin (10 mg/kg PO; Viatris, Canonsburg, PA, USA), and tramadol (10 mg/kg PO; Yuhan).

Clinical evaluations were performed at 1, 2, 4, and 8 weeks postoperatively. Lameness was

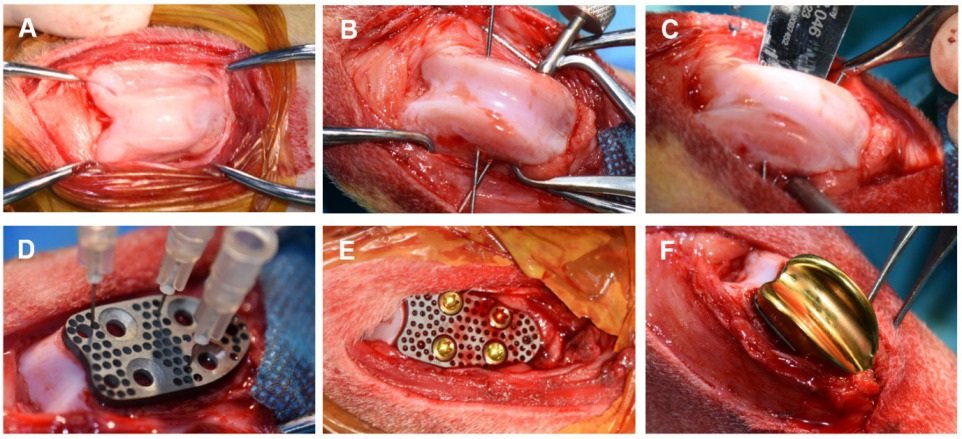

Fig. 2. Surgical procedure for implantation of the PGR system in the canine stifle joint. (A) Exposure of the patellar groove. (B) Placement of two Kirschner wires 2 mm below the groove to guide osteotomy. (C) Removal of the native trochlear groove using an oscillating saw. (D) Positioning of the base plate and temporary fixation with 26G syringe needles. (E) Final fixation with cortical screws. (F) Locking of the artificial patellar groove onto the base plate. PGR, patellar groove replacement.

https://doi.org/10.12729/jbtr.2025.26.4.107

graded on a 0–4 scale (0 = normal gait; 1 = mild, intermittent; 2 = persistent, moderate; 3 = severe; 4 = non-weight-bearing) according to the criteria described by Dokic et al. [13]. Physical examination at 4 and 8 weeks assessed crepitus, range of motion (ROM), joint effusion, pain, and stifle stability.

Fluoroscopic images were obtained immediately after surgery, at 1, 2, 4, and 8 weeks, and at 6 and 12 months using a flat-panel detector C-arm system (OSCAR Prime, GENORAY, Seoul, Korea; 60 kVp, 1.6 mA, pulse mode 8 frames/s). Computed tomography (CT) scans were performed at 8 weeks, 6 months, and 1 year under general anesthesia (Incisive CT, Philips, Amsterdam, Netherlands; 140 kVp, 100 mAs). At 1 year, magnetic resonance imaging (MRI; 3.0 T, Achieva, Philips Healthcare, Best, The Netherlands) was performed using a T2-weighted fast spin-echo sequence (TR 3,000 ms; TE 100 ms; slice thickness 3.0 mm) with a dedicated stifle coil to evaluate patellofemoral alignment and periarticular soft tissues.

Micro-computed tomography analysis

At the 1-year observation period, both dogs were humanely euthanized by intravenous administration of potassium chloride (KCl-40, Dai Han Pharm, Seoul, Korea) under deep anesthesia. The distal femurs containing the implants were harvested for micro-CT analysis (SkyScan 1273, Bruker, Kontich, Belgium) performed at 100 kV, 40 μA, and 0.5° rotation steps using an Al + Cu filter (1 mm + 0.038 mm). Images were reconstructed using NRecon software (Bruker) to assess bone–implant integration, peri-implant bone formation, and potential osteolytic changes.

RESULTS

Physicochemical property tests

The results of physicochemical characterization are summarized in Table 1. In the neutral salt spray test, both ADLC- and TiN-coated samples exhibited excellent corrosion resistance, showing no signs of surface oxidation or discoloration after 96 hours of exposure.

In hardness testing, ADLC-coated samples demonstrated an average indentation hardness (HIT) of 29.15 ± 0.96 GPa and Vickers hardness (HVIT) of 2,700 ± 85 HV, whereas TiN-coated samples exhibited significantly higher values (HIT: 32.07 ± 0.84 GPa, HVIT: 2,970 ± 92 HV, * $p<0.05$).

Table 1. Data from physicochemical tests of implant materials

Coating type	Neutral salt spray test	Indentation hardness (GPa)	Surface roughness test (μmRa)	Coating thickness test (μm)
ADLC-coated implant	Negative (no corrosion)	29.15 ± 0.96	0.10 ± 0.01	1.56 ± 0.03
TiN-coated implant	Negative (no corrosion)	32.07 ± 0.84*	0.09 ± 0.01	1.71 ± 0.02*

Indicates a statistically significant difference compared with ADLC-coated implants (* $p<0.05$). Both coatings exhibited excellent corrosion resistance. TiN-coated implants showed greater hardness and coating thickness. The surface roughness of the two coatings was comparable.

* Values are presented as the mean ± S.D. (n=5).

ADLC, amorphous diamond-like carbon; TiN, titanium nitride.

The surface roughness characteristics of the two coatings were comparable, with each showing different strengths. While the TiN-coated implants exhibited a slightly lower average roughness (Ra = 0.09 ± 0.01 μm vs. 0.10 ± 0.01 μm), the ADLC-coated implants showed a lower maximum roughness height (Rz = 1.05 ± 0.04 μm vs. 1.36 ± 0.06 μm), indicating fewer extreme peaks and valleys. Coating thickness ranged from 1.53–1.59 μm for ADLC and 1.69–1.73 μm for TiN, with the TiN group exhibiting a significantly thicker and more uniform layer ($^{*}p<0.05$).

Collectively, these findings indicate that both coatings possess robust physicochemical stability, while TiN coatings provide superior hardness and coating integrity, supporting their mechanical reliability and potential for mass production.

In vitro evaluation of implants

Cytotoxicity test

Negative control extracts yielded a mean cell viability of 75.34 ± 2.1%, while positive control extracts produced a clear dose-dependent cytotoxicity (≤ 70%), confirming test validity. Both ADLC- and TiN-coated samples maintained cell viability above 90% across all concentrations, indicating the absence of cytotoxic effects. TiN-coated extracts showed slightly higher cell viability (up to 113.6 ± 2.8%) than those from ADLC-coated samples (up to 110.9 ± 3.2%), although the difference was not statistically significant (Figs. 3 and 4). These results confirm that neither coating induces cytotoxicity, and TiN exhibits excellent cellular compatibility comparable to ADLC.

Cell adhesion and proliferation

At 4 hours, cell adhesion was lower on TiN-coated surfaces (1.5 ± 0.1 × 10^3 cells) compared with uncoated Ti-6Al-4V surfaces (2.5 ± 0.2 × 10^3 cells) and stainless steel control surfaces (7.5 ± 0.4 × 10^3 cells). However, at 24 hours, no difference in proliferation was observed between TiN-coated and uncoated samples (≈ 2.0 × 10^3 cells). These findings suggest that TiN's dense, low-energy surface initially limits adhesion but does not inhibit subsequent cell proliferation, supporting its suitability for long-term implant–tissue contact.

In vivo inflammatory response in rats

The untreated control group exhibited plasma IL-1β and IL-6 levels of 3.79 ± 0.22 pg/mL and 4.12 ± 0.25 pg/mL, respectively. The ADLC-coated group showed slightly lower levels (IL-1β: 2.72 ± 0.18 pg/mL; IL-6: 2.58 ± 0.16 pg/mL), while TiN-coated samples exhibited comparable results (IL-1β: 3.72 ± 0.20 pg/mL; IL-6: 3.32 ± 0.19 pg/mL). No statistically significant differences were observed between groups ($p>0.05$), indicating that both coatings elicited minimal systemic inflammatory responses.

Overall, the TiN coating demonstrated comparable *in vivo* biocompatibility to ADLC, without evidence of pro-inflammatory cytokine activation.

https://doi.org/10.12729/jbtr.2025.26.4.107

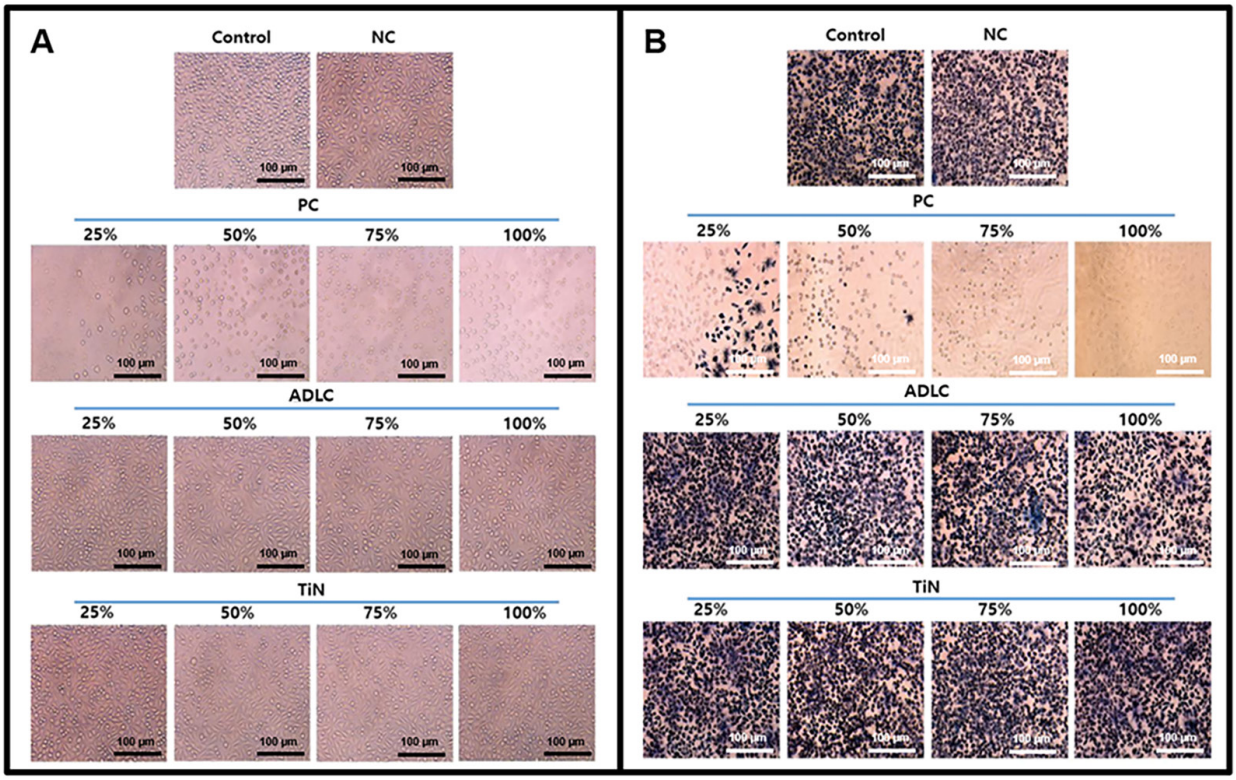

Fig. 3. Representative L-929 cell morphology during the cytotoxicity test of coated materials (× 200). (A) Cells after exposure to material extracts. (B) Cells following MTT treatment. No visible differences were observed between the ADLC- and TiN-coated sample groups. NC, negative control; PC, positive control; ADLC, amorphous diamond-like carbon group; TiN, titanium nitride group.

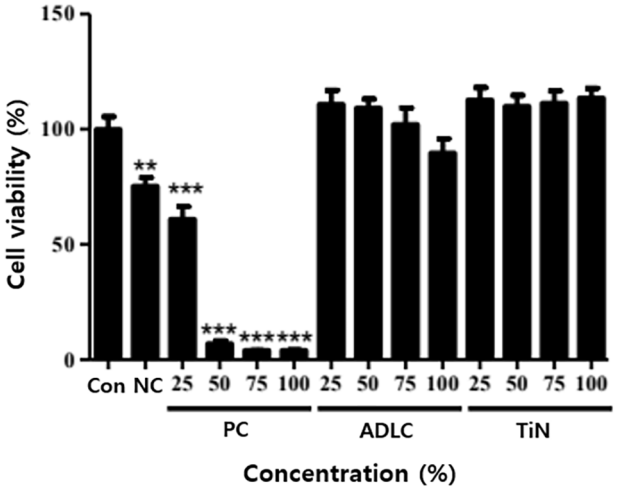

Fig. 4. Cell viability of L-929 fibroblasts in the MTT cytotoxicity test. Both ADLC and TiN coatings maintained cell viabilities above 80% at all extract concentrations, indicating no cytotoxic potential. Data are expressed as the mean ± S.E. (n = 5). Statistical analysis was performed using one-way ANOVA. $^{**}p<0.01$, $^{***}p<0.001$ vs. control. Con, control; NC, negative control; PC, positive control; ADLC, amorphous diamond-like carbon; TiN, titanium nitride.

In vivo preclinical study in dogs

Gait analysis

Both dogs exhibited transient postoperative lameness that improved progressively and resolved within 4 weeks.

- Dog 1: Grade 2 lameness at week 1 → Grade 1 at week 2 → Normal gait by week 4.
- Dog 2: Grade 2 lameness at week 1 → Grade 1 by week 4 → Full recovery by week 8.

This rapid recovery suggests favorable joint adaptation and implant stability.

Physical examination

At 4 weeks, Dog 1 exhibited normal joint function without crepitus (ROM: 170°/47° right, 168°/45° left), while Dog 2 showed transient bilateral crepitus (171°/48° and 171°/46°). By 8 weeks, both dogs demonstrated near-normal ROM with no effusion, pain, or instability. These findings indicate that both TiN- and ADLC-coated implants supported physiological joint motion without eliciting mechanical irritation.

Radiologic and imaging evaluations

Fluoroscopic images obtained immediately after implantation revealed minor gaps at the bone–implant interface, which resolved by week 8, confirming stable fixation. At 6 months and 1 year, no implant loosening, bone resorption, or pathological changes were detected (Fig. 5). CT and MRI analyses at 8 weeks, 6 months, and 1 year confirmed proper patellofemoral alignment and smooth articulation between the artificial groove and patella. MRI at 1 year demonstrated intact quadriceps and patellar tendons, no joint effusion, and no abnormal synovial proliferation (Fig. 6). These imaging findings verify long-term implant stability, accurate alignment, and soft-tissue compatibility.

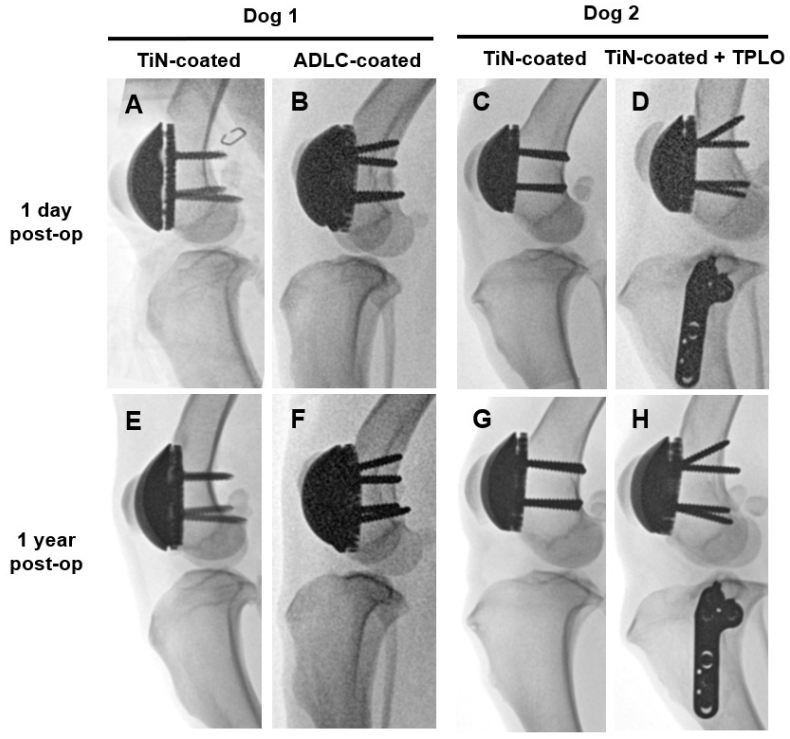

Fig. 5. Serial fluoroscopic images of canine stifle joints obtained 1 day (A–D) and 1 year (E–H) after PGR implantation. (A, E) TiN-coated implant (Dog 1, right stifle), (B, F) ADLC-coated implant (Dog 1, left stifle), (C, G) TiN-coated implant (Dog 2, right stifle), (D, H) TiN-coated implant combined with TPLO (Dog 2, left stifle). All implants remained well positioned without loosening, migration, or peri-implant abnormalities throughout the follow-up period. TiN, titanium nitride; ADLC, amorphous diamond-like carbon; TPLO, tibial plateau leveling osteotomy; PGR, patellar groove replacement.

https://doi.org/10.12729/jbtr.2025.26.4.107

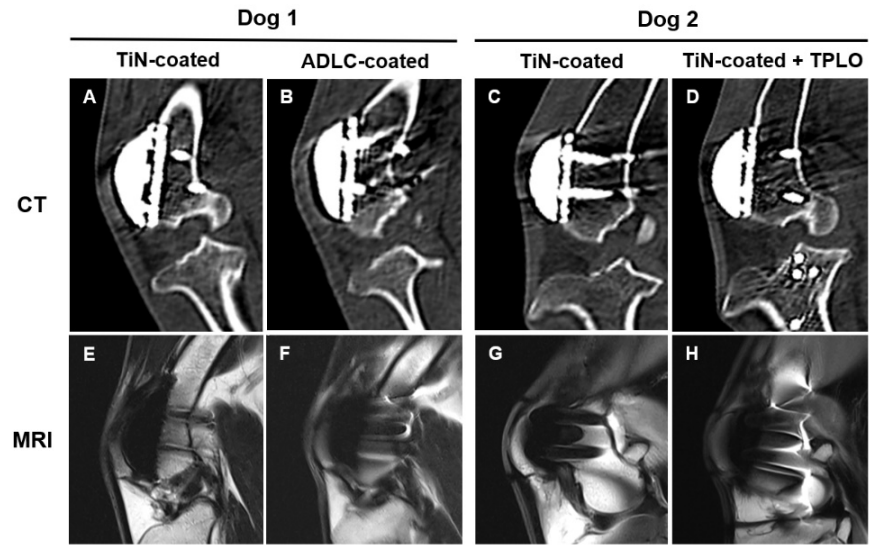

Fig. 6. Computed tomography (CT) and magnetic resonance imaging (MRI) of stifle joints 1 year after implantation. (A–D) Sagittal CT reconstructions, selected because this plane optimally demonstrates patellofemoral alignment and screw/pin tracts for loosening assessment: (A) TiN (Dog 1, right), (B) ADLC (Dog 1, left), (C) TiN (Dog 2, right), (D) TiN + TPLO (Dog 2, left). (E–H) Sagittal T2-weighted fast spin-echo MRI (TR 3,000 ms; TE 100 ms; slice 3.0 mm) obtained with a dedicated stifle coil to evaluate joint capsule and periarticular soft tissues: (E) TiN (Dog 1, right), (F) ADLC (Dog 1, left), (G) TiN (Dog 2, right), (H) TiN + TPLO (Dog 2, left). Soft-tissue structures were normal in all MRI panels. TiN, titanium nitride; ADLC, amorphous diamond-like carbon; TPLO, tibial plateau leveling osteotomy.

Micro-computed tomography assessment

Postmortem micro-CT evaluation at 1 year demonstrated well-developed peri-implant trabecular bone and intimate bone–implant contact in both coating groups. No evidence of osteolysis, fibrous encapsulation, or interfacial gaps was observed (Fig. 7). Bone volume and density around TiN-coated implants were comparable to those of ADLC, confirming excellent

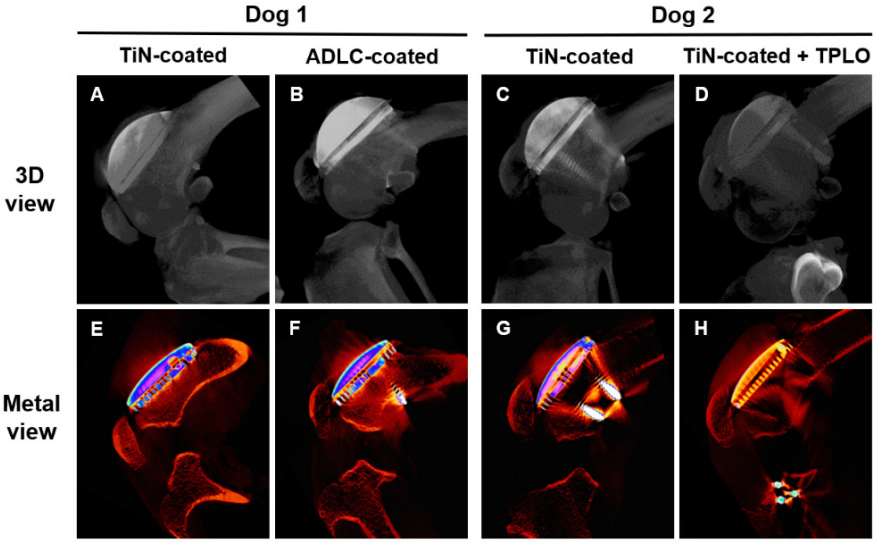

Fig. 7. Sagittal micro-CT evaluation 1 year after PGR implantation. (A–D) 3D sagittal reconstructions showing overall implant positioning: (A) TiN (Dog 1, right), (B) ADLC (Dog 1, left), (C) TiN (Dog 2, right), (D) TiN + TPLO (Dog 2, left). (E–H) Metal-enhanced sagittal views highlighting the bone–implant interface and fixation quality for the same sequence of implants. Across all panels, both coatings demonstrate intimate bone–implant contact without radiolucency, osteolysis, or interfacial gaps, with satisfactory peri-implant trabecular bone formation. TiN, titanium nitride; ADLC, amorphous diamond-like carbon; TPLO, tibial plateau leveling osteotomy; CT, computed tomography; PGR, patellar groove replacement.

osteointegration and mechanical stability.

DISCUSSION

PGR has recently emerged as a salvage option for managing advanced MPL, especially in dogs with severe femoropatellar osteoarthritis or those unresponsive to conventional techniques. Traditional surgical procedures, such as trochleoplasty or tibial tuberosity transposition, are generally effective for low-grade MPL but are often inadequate for advanced cases associated with angular deformities or chronic degenerative changes. In such situations, PGR provides a prosthetic trochlear groove that restores patellar tracking along a biomechanically stable pathway, thereby reducing pain and preserving joint mobility [11–15].

The TiN-coated PGR system developed in this study was not intended to surpass the ADLC-coated predicate device in all aspects but to achieve comparable biological and mechanical performance while offering practical advantages in manufacturability, coating adhesion, and production cost. Unlike the CNC machining and multi-step PACVD processes required for ADLC coating—which typically involve adhesion interlayers and hydrocarbon gas activation—the TiN-coated prototypes were fabricated using injection molding followed by arc ion plating performed at approximately 300°C–350°C and 0.1–0.2 Pa in a single-stage deposition cycle. Previous comparative studies have also shown that TiN coatings exhibit higher scratch-adhesion strength (Lc3 ≈ 16.5 N) than DLC coatings (Lc3 ≈ 10.6 N), suggesting more robust coating stability under simpler processing conditions [29]. These quantitative differences support the scalability and cost-efficiency of TiN manufacturing, enabling potential transition of PGR systems from specialized applications to broader clinical use.

Physicochemical evaluation confirmed that both coatings provided high corrosion resistance and surface integrity. However, TiN demonstrated greater hardness and thicker, more uniform coating layers, indicating enhanced wear resistance and coating stability, which is consistent with previous reports describing the strong correlation between coating hardness, structural uniformity, and abrasion resistance in nitride-based hard coatings [30]. The surface roughness profiles were comparable, though distinct. The lower average roughness (Ra) of the TiN coating is advantageous for reducing overall friction, while the lower maximum roughness height (Rz) of the ADLC surface suggests a more uniform topography with fewer potential initiation sites for wear. These interpretations are supported by studies showing that increased Ra or Rz values elevate asperity-induced stress concentration and promote earlier fatigue crack initiation under cyclic loading [31].

Biological assessments further verified that both coatings were non-cytotoxic and biocompatible, with TiN showing slightly higher cell viability and no inhibition of cell proliferation. The transient reduction in cell adhesion on TiN surfaces likely reflects the coating's low surface energy rather than any cytotoxicity, aligning with previous findings in orthopedic and dental applications [23–25]. *In vivo* studies in rats confirmed the absence of significant systemic inflammatory cytokine responses (IL-1β and IL-6), supporting the systemic safety of both materials. It should be noted that only systemic cytokines were evaluated in this feasibility study; local tissue-level

https://doi.org/10.12729/jbtr.2025.26.4.107

inflammatory responses—typically assessed using markers such as TNF-α, macrophage infiltration, or periprosthetic histology—were not measured and will be incorporated in future studies to provide a more comprehensive assessment of local biomaterial reactivity.

Preclinical evaluation in beagles demonstrated successful implantation, stable fixation, and restoration of normal gait within weeks postoperatively. Radiographic and advanced imaging analyses (CT, MRI, and micro-CT) confirmed proper patellofemoral alignment, satisfactory bone–implant integration, and intact surrounding soft tissues without pathological findings. These findings are consistent with recent imaging-based methods for evaluating bone–implant integration [32–34]. Although clinical lameness grading and multimodal imaging were sufficient for confirming functional recovery in this feasibility study, objective gait analysis such as quantitative weight-bearing assessment was not performed; incorporating kinetic measurements will strengthen future evaluations. In Dog 2, TiN-coated implants were intentionally combined with TPLO to evaluate performance under a more complex surgical condition. Although an ADLC+TPLO group would have provided an additional comparator, ADLC-coated implants are already clinically established with well-documented safety, and the present study prioritized assessing the newer TiN system under both standard and combined procedures. Collectively, these results indicate that the TiN-coated PGR system shows clinical outcomes comparable to those of the ADLC-coated device while offering manufacturing and cost advantages that may enhance accessibility for general veterinary practice.

From a clinical and industrial standpoint, the TiN-coated PGR system represents a practical alternative for treating severe MPL and other femoropatellar disorders. The cost-efficiency and scalability of the injection molding and arc ion plating processes can significantly reduce manufacturing expenses and enable customized or mass-produced implants for a wider range of companion animal patients. This improvement could help transition PGR procedures from a niche, high-cost solution to a standardized and economically viable therapy in veterinary orthopedics.

However, this study has several limitations, including the small number of animals and a relatively short follow-up period. While early outcomes were favorable, long-term studies evaluating wear resistance, coating delamination, and fatigue performance are necessary to validate durability under prolonged biomechanical stress. Additionally, because postoperative assessments relied on fluoroscopic imaging rather than static digital radiography, geometric accuracy was reduced, motion-related distortion was possible, and bone density measurements could not be reliably obtained, which should be considered when interpreting peri-implant features. Comparative analyses with other advanced coatings such as hydroxyapatite, porous titanium, or hybrid multilayer films may further elucidate optimization strategies for future implant systems. Ultimately, randomized controlled clinical trials in dogs with naturally occurring MPL will be essential to confirm the translational relevance and establish clinical guidelines for TiN-coated PGR use in veterinary practice.

Conclusion

This study comprehensively evaluated TiN- and ADLC-coated PGR systems to identify an optimal surface coating for veterinary orthopedic applications. Both coatings exhibited ex-

cellent physicochemical stability, corrosion resistance, and biocompatibility, confirming their suitability for long-term implantation.

The TiN-coated system demonstrated greater hardness, thicker and more uniform coating layers, and comparable biological safety to the ADLC-coated device. Importantly, the TiN coating can be produced through injection molding combined with arc ion plating, which requires simpler equipment, lower processing temperatures, and reduced manufacturing costs compared with the CNC machining and vacuum deposition methods used for ADLC.

Preclinical implantation in beagles confirmed that the TiN-coated PGR system provided stable fixation, satisfactory patellar alignment, preserved joint motion, and excellent bone–implant integration without adverse tissue reactions.

Collectively, these results indicate that TiN-coated PGR systems achieve equivalent biological and mechanical performance to those of ADLC-coated devices while offering distinct advantages in manufacturability, cost-efficiency, and clinical scalability. TiN surface coating thus represents a promising, practical, and economically viable solution for next-generation veterinary orthopedic implants and may facilitate the broader clinical adoption of PGR procedures in managing severe MPL.

Future work should include long-term durability testing, fatigue and wear analyses, and controlled clinical trials in dogs with naturally occurring MPL to further validate the translational and commercial potential of TiN-coated PGR implants.

REFERENCES

1. Bound N, Zakai D, Butterworth SJ, Pead M. The prevalence of canine patellar luxation in three centres. Vet Comp Orthop Traumatol 2009;22:32-37.
2. LaFond E, Breur GJ, Austin CC. Breed susceptibility for developmental orthopedic diseases in dogs. J Am Anim Hosp Assoc 2002;38:467-477.
3. Ness MG, Abercromby RH, May C, Turner BM, Carmichael S. A survey of orthopaedic conditions in small animal veterinary practice in Britain. Vet Comp Orthop Traumatol 1996;09:43-52.
4. Brinker WO, Pierrmattei DL, Flo GL. Diagnosis and treatment of orthopedic conditions of the hindlimb. In: Brinker WO, Pierrmattei DL, Flo GL (eds.). Brinker, Piermattei and Flo's handbook of small animal orthopedics and fracture treatment. 2nd ed. Philadelphia: Elsevier Saunders; 1990. p. 377-397.
5. Roush JK. Canine patellar luxation. Vet Clin North Am Small Anim Pract 1993;23:855-868.
6. Linney WR, Hammer DL, Shott S. Surgical treatment of medial patellar luxation without femoral trochlear groove deepening procedures in dogs: 91 cases (1998–2009). J Am Vet Med Assoc 2011;238:1168-1172.
7. Slocum B, Slocum TD. Trochlear wedge recession for medial patellar luxation. Vet Clin North Am Small Anim Pract 1993;23:869-875.
8. Arthurs GI, Langley-Hobbs SJ. Complications associated with corrective surgery for patellar luxation in 109 dogs. Vet Surg 2006;35:559-566.

https://doi.org/10.12729/jbtr.2025.26.4.107

9. Kowaleski MP, Boudrieau RJ, Pozzi A. Stifle joint. In: Tobias KM, Johnston SA (eds.). Veterinary surgery: small animal. 1st ed. Philadelphia: Elsevier Saunders; 2012. p. 973-988.
10. Swiderski JK, Palmer RH. Long-term outcome of distal femoral osteotomy for treatment of combined distal femoral varus and medial patellar luxation: 12 cases (1999–2004). J Am Vet Med Assoc 2007;231:1070-1075.
11. Chase D, Farrell M. Fracture of the lateral trochlear ridge after surgical stabilisation of medial patellar luxation. Vet Comp Orthop Traumatol 2010;23:203-208.
12. Ostberg SE, Dimopoulou M, Lee MH. Ilial crest bone graft transposition as treatment for fracture of the medial femoral trochlear ridge in a dog. Vet Comp Orthop Traumatol 2014;27:80-84.
13. Dokic Z, Lorinson D, Weigel JP, Vezzoni A. Patellar groove replacement in patellar luxation with severe femoro-patellar osteoarthritis. Vet Comp Orthop Traumatol 2015;28:124-130.
14. Oană LA. A surgical technique of medial patellar luxation in dogs. Bull Univ Agric Sci Vet Med Cluj-Napoca Vet Med 2010;67:6031.
15. Pinna S, Venturini A, Tribuiani AM. Rotation of the femoral trochlea for treatment of medial patellar luxation in a dog. J Small Anim Pract 2008;49:163-166.
16. Fedel M. Blood compatibility of diamond-like carbon (DLC) coatings. In: Narayan R (ed.). Diamond-based materials for biomedical applications. Sawston: Woodhead; 2013. p. 71-102.
17. Love CA, Cook RB, Harvey TJ, Dearnley PA, Wood RJK. Diamond like carbon coatings for potential application in biological implants: a review. Tribol Int 2013;63:141-150.
18. Singh A, Ehteshami G, Massia S, He J, Storer RG, Raupp G. Glial cell and fibroblast cytotoxicity study on plasma-deposited diamond-like carbon coatings. Biomaterials 2003;24:5083-5089.
19. Choudhury D, Lackner J, Fleming RA, Goss J, Chen J, Zou M. Diamond-like carbon coatings with zirconium-containing interlayers for orthopedic implants. J Mech Behav Biomed Mater 2017;68:51-61.
20. Alakoski E, Tiainen VM, Soininen A, Konttinen YT. Load-bearing biomedical applications of diamond-like carbon coatings - current status. Open Orthop J 2008;2:43-50.
21. Makarov V, Strel'nitskij V, Dedukh N, Nikolchenko O. Diamond-like carbon coatings in endoprosthetics (literature review). Orthop Traumatol Prosthet 2019;2:102-111.
22. Hauert R. A review of modified DLC coatings for biological applications. Diam Relat Mater 2003;12:583-589.
23. AbuAlia M, Fullam S, Cinotti F, Manninen N, Wimmer MA. Titanium nitride coatings on Co-CrMo and Ti6Al4V alloys: effects on wear and ion release. Lubricants 2024;12:96.
24. Alexander JS, Hurst JM, Morris MJ. Use of ion beam enhanced deposition (IBED) titanium nitride for knee arthroplasty implants. Surg Technol Int 2023;42:239-243.
25. Shenhar A, Gotman I, Radin S, Ducheyne P, Gutmanas EY. Titanium nitride coatings on surgical titanium alloys produced by a powder immersion reaction assisted coating method: residual stresses and fretting behavior. Surf Coat Technol 2000;126:210-218.
26. Grądzka-Dahlke M. Comparison of functional properties of thin layers on titanium and cobalt implant alloys. Defect Diffusion Forum 2010;297-301:1053-1058.

27. Yuan Z, He Y, Lin C, Liu P, Cai K. Antibacterial surface design of biomedical titanium materials for orthopedic applications. J Mater Sci Technol 2021;78:51-67.
28. Pawlik M, Trębacz P, Barteczko A, Kurkowska A, Piątek A, Paszenda Z. Evaluation of patellar groove prostheses in veterinary medicine: review of technological advances, technical aspects, and quality standards. Materials 2025;18:1652.
29. Łępicka M, Grądzka-Dahlke M, Pieniak D, Pasierbiewicz K, Niewczas A. Effect of mechanical properties of substrate and coating on wear performance of TiN- or DLC-coated 316LVM stainless steel. Wear 2017;382–383:62-70.
30. Musil J. Hard and superhard nanocomposite coatings. Surf Coat Technol 2000;125:322-330.
31. Azari S, Papini M, Spelt JK. Effect of surface roughness on the performance of adhesive joints under static and cyclic loading. J Adhes 2010;86:742-764.
32. Gausper A, Gibbs WN, Elder BD, Scheer JK, Perry TG, Etigunta SK, Liu AM, Tuchman A, Walker CT. Magnetic resonance imaging-based assessment of bone quality using vertebral bone quality (VBQ) scores in spine surgery: a critical assessment and narrative review. J Clin Med 2025;14:6477.
33. Woisetschläger M, Booij R, Tesselaar E, Oei EHG, Schilcher J. Improved visualization of the bone-implant interface and osseointegration in *ex vivo* acetabular cup implants using photon-counting detector CT. Eur Radiol Exp 2023;7:19.
34. Booij R, de Klerk P, Tesselaar E, Woisetschläger M, Brandts A, Olsthoorn M, van Oldenrijke J, Bose K, Schilcherb J, Oeia EHG. Assessment of bone-implant interface image quality for *in-vivo* acetabular cup implants using photon-counting detector CT: impact of tin pre-filtration. Eur J Radiol Open 2025;14:100646.

https://doi.org/10.12729/jbtr.2025.26.4.107